

The public reporting burden for this collection of information is estimated to average 1 hour per response, including the time for reviewing instructions, searching existing data sources, gathering and maintaining the data needed, and completing and reviewing the collection of information. Send comments regarding this burden estimate or any other aspect of this collection of information, including suggestions for reducing this burden, to Washington Headquarters Services, Directorate for Information Operations and Reports, 1215 Jefferson Davis Highway, Suite 1204, Arlington VA, 22202-4302. Respondents should be aware that notwithstanding any other provision of law, no person shall be subject to any penalty for failing to comply with a collection of information if it does not display a currently valid OMB control number.
PLEASE DO NOT RETURN YOUR FORM TO THE ABOVE ADDRESS.

1. REPORT DATE (DD-MM-YYYY)	2. REPORT TYPE Technical Report	3. DATES COVERED (From - To) -
-----------------------------	------------------------------------	-----------------------------------

4. TITLE AND SUBTITLE Taming the complexity of granular materials with vector calculus	5a. CONTRACT NUMBER W911NF-07-1-0370
	5b. GRANT NUMBER
	5c. PROGRAM ELEMENT NUMBER 611102

6. AUTHORS A. Tordesillas, D. Kirszenblat, C. Mangelsdorf	5d. PROJECT NUMBER
	5e. TASK NUMBER
	5f. WORK UNIT NUMBER

7. PERFORMING ORGANIZATION NAMES AND ADDRESSES University of Melbourne Melbourne Research Swanston Street	8. PERFORMING ORGANIZATION REPORT NUMBER
--------------------------------------------------------------------------------------------------------------------	------------------------------------------

9. SPONSORING/MONITORING AGENCY NAME(S) AND ADDRESS (ES) U.S. Army Research Office P.O. Box 12211 Research Triangle Park, NC 27709-2211	10. SPONSOR/MONITOR'S ACRONYM(S) ARO
	11. SPONSOR/MONITOR'S REPORT NUMBER(S) 51924-EV.23

12. DISTRIBUTION AVAILABILITY STATEMENT Approved for public release; distribution is unlimited.

13. SUPPLEMENTARY NOTES The views, opinions and/or findings contained in this report are those of the author(s) and should not be construed as an official Department of the Army position, policy or decision, unless so designated by other documentation.

14. ABSTRACT Granular materials, which occur widely in nature and industry, exhibit a vast range of complex behaviour: self-organised pattern formation and multiphase behaviour that defies conventional solid/ fluid/ gas classification. Arguably the most important source of this complexity is the immense number of degrees of freedom in the system, an aspect that presents serious challenges to the modeller. In particular, the fundamental continuum mechanics concept of strain, the mathematical quantity used to describe how a material deforms, cannot adequately describe the motion of even the smallest particle cluster. In this paper, we demonstrate how key concepts from vector

15. SUBJECT TERMS nonaffine deformation, vector calculus, granular media

16. SECURITY CLASSIFICATION OF:	17. LIMITATION OF ABSTRACT	15. NUMBER OF PAGES	19a. NAME OF RESPONSIBLE PERSON Antoinette Tordesillas
a. REPORT UU	b. ABSTRACT UU	c. THIS PAGE UU	19b. TELEPHONE NUMBER 038-344-9685

Report Title

Taming the complexity of granular materials with vector calculus

ABSTRACT

Granular materials, which occur widely in nature and industry, exhibit a vast range of complex behaviour: self-organised pattern formation and multiphase behaviour that defies conventional solid/ fluid/ gas classification. Arguably the most important source of this complexity is the immense number of degrees of freedom in the system, an aspect that presents serious challenges to the modeller. In particular, the fundamental continuum mechanics concept of strain, the mathematical quantity used to describe how a material deforms, cannot adequately describe the motion of even the smallest particle cluster. In this paper, we demonstrate how key concepts from vector calculus can be used to formulate and model complex particle motions that hold the key to understanding the deformation, failure and flow of granular materials. We present a number of examples to facilitate the implementation of these concepts in lectures. A code in Excel has been written to enable an exploration of a wide range of particle motions, and to provide an invaluable tool for designing problems for students to work on in assignments.

Taming the complexity of granular materials with vector calculus *

A Tordesillas †, D Kirszenblat and C Mangelsdorf
Department of Mathematics and Statistics, The University of Melbourne, Victoria

SUMMARY: *Granular materials, which occur widely in nature and industry, exhibit a vast range of complex behaviour: self-organised pattern formation and multiphase behaviour that defies conventional solid/fluid/gas classification. Arguably the most important source of this complexity is the immense number of degrees of freedom in the system, an aspect that presents serious challenges to the modeller. In particular, the fundamental continuum mechanics concept of strain, the mathematical quantity used to describe how a material deforms, cannot adequately describe the motions of even the smallest particle cluster. In this paper, we demonstrate how key concepts from vector calculus can be used to formulate and model complex particle motions that hold the key to understanding the deformation, failure and flow of granular materials. We present a number of examples to facilitate the implementation of these concepts in lectures. A code in Excel has been written to enable an exploration of a wide range of particle motions, and to provide an invaluable tool for designing problems for students to work on in assignments.*

1 INTRODUCTION

This paper concerns the mathematical modelling of the deformation of granular materials. It showcases modern applications of undergraduate-level vector calculus in the context of evolving vector fields – specifically, the study of the kinematics (displacements, rotations and velocities) of an assembly of “grains” as they engage in self-organised pattern formation.

Granular materials form a class of materials encompassing everything from soil and natural grains to pharmaceutical pills and chemical powders. They are ubiquitous in nature and commercially vital in many industries such as chemical, agricultural, cosmetics, food manufacturing, pharmaceutical and mining industries (see figure 1). Considered as the ultimate paradigm of complex systems, granular materials exhibit emergent behaviour that has eluded scientists for centuries. Today, there is still no universally-accepted constitutive model to predict how granular materials will behave under load. Consequently, systems and processes involving granulates rarely reach 60% of their design capacity, whereas processes involving fluids operate on

average at 96% design capacity (Duran, 2000; Oda & Iwashita, 2005). Thus, even a fractional advance in our understanding of how granular media behave can have a profound economic and social impact.

Numerous models of granular materials are constructed within the framework of classical continuum theory (Oda & Iwashita, 2005). This theory is based on the assumption that the body is continuous and comprises material points that bear only translational degrees of freedom. By contrast, a granular material is a discrete assembly of solid particles, each of which has translational as well as rotational degrees of freedom. Classical continuum mechanics asserts that a material should undergo homogeneous or affine deformation in response to homogeneous boundary forces, that is, the change in shape of the material should be uniform throughout the whole material. Therefore, in an affine deformation the components of the strain tensor are independent of position (ie. are constants or functions of time only). But experiments have shown that a granular material subjected to uniform boundary forces exhibits significant non-affine deformation, ie. local deviations from affine deformation (see, for example, Tordesillas et al (2009) and references therein). Non-affine deformation becomes particularly important during self-organised pattern formation, a common phenomenon that arises almost from the onset of loading, especially in densely packed granular systems (LTB Group, 2004;

* Paper D09-EM08 submitted 16/06/09; accepted for publication after review and revision 29/07/09.

† Corresponding author A/Prof Antoinette Tordesillas can be contacted at atordes@ms.unimelb.edu.au.



Figure 1: Granular materials are part of everyday life. Catastrophic failures (eg. collapse of silo and road failure) are frequent (For movies and images of force chains from experiments, visit www.phy.duke.edu/~bob).

Behringer, n. d.; Duran, 2000; Oda & Iwashita, 2005; Tordesillas et al, 2008; 2009; Tordesillas & Arber, 2005; Majmudar & Behringer, 2005; Rechenmacher, 2006; Oda et al, 2004; Kuhn & Bagi, 2002; Mueth et al, 2000; Tordesillas, 2007).

By far the most striking example of emergent pattern formation in a deforming granular medium resides in the manner by which the material transmits force via a dual complex force network, as shown in figure 2. The first, known as the strong network, comprises force chains: quasi-linear particle chains through which above average contact forces are transmitted (LTB Group, 2004; Behringer, n. d.; Majmudar & Behringer, 2005). The second, known as the weak network, comprises the remaining particles bearing relatively small forces: these surround and provide lateral stability to the force chains. Force chains may span only a few grains in length, or they may extend for hundreds of grain diameters. Physical experiments using techniques of photo-elasticity have shown that force chains align themselves in the direction where the material feels the greatest compression (Oda & Iwashita, 2005; Tordesillas et al, 2009). In essence then force chains are emergent columnar structures that are subject to axial compression. As the material deforms under load, the temporal evolution of these force chains is one characterised by the continual birth of new force chains and collapse by buckling of old force chains. This evolution is highly non-affine, and involves large rotations and gradients in rotations¹ (for movies of shear band evolution in a granular media simulation, visit www.mgm.ms.unimelb.edu.au/projects2009.php). Experiments and numerical simulations have shown that failure to capture this aspect in constitutive modelling results in poor predictive capabilities (see Tordesillas et al (2008; 2009) and references cited therein for more details).

¹ The movie of the photo-elastic disc experiment shows the development of rotating mesoscopic clusters highlighting the multiscale nature of pattern formation in these systems.

Vector and tensor calculus is currently taught to second- and third-year undergraduate mathematics, physics and engineering students. Typically, basic operations and concepts such as divergence, curl, vector fields, flow lines, etc. are explained physically using fluid flow. In this paper, we demonstrate how vector and tensor calculus can be applied at the cutting edge of research in the science of complex media to quantify the non-affine deformation of granular materials. Attention is paid to the "transition regime" during which the material effectively undergoes a phase change from solid-like to liquid-like behaviour. This has proven to be one of the most challenging regimes from the standpoint of mathematical modelling, as the material self-organises to form failure patterns at multiple length scales (eg. microbands, force chain buckling, shear band) (Tordesillas et al, 2008; 2009; Rechenmacher, 2006; Oda et al, 2004; Kuhn & Bagi, 2002; Mueth et al, 2000; Tordesillas, 2007). A simple computer code for calculating the non-affine deformation associated with the deformation of a particle cluster can readily be implemented in an Excel spreadsheet (available from the authors upon request).

2 DEFORMATION OF A CONTINUUM

In general, the application of force to a continuous body gives rise to a combination of rigid body motion and a change in shape of the body. The change in shape is called deformation. Deformable bodies can change shape, whereas rigid bodies can only undergo rigid-body motions. We now briefly review the deformation of a classical continuum body, as typically presented in the introductory sections of a classical solid mechanics textbook (eg. Hjeltnstad, 2005).

To quantify deformation, we must completely characterise the initial geometry of the body B . We may treat this initial geometry B as the reference configuration. The reference configuration has two



Figure 2: Images of bright chains of photo-elastic particles carrying above average forces, ie. “force chains”, existing amidst dark particles which carry small or zero forces. From top right clockwise are images of force transmission patterns in granular assemblies: (a) sheared between concentric cylinders (outer cylinder is fixed, inner cylinder is rotating); (b) under an “impacting” steel ball; (c) close-up view of stress pattern in individual particles; and (d) in an exhibit at the Chicago Museum of Science and Industry by R. P. Behringer (LTB Group, 2004; Behringer, n. d.).

basic features: the domain B , which is the interior of the body, and the boundary S , which is the surface of the body. The first assumption in continuum mechanics is that we know the position of every point in the body in the reference configuration. We can then locate the position of a point P by assigning it a position vector \mathbf{x} with coordinates (x_1, x_2, x_3) . The second assumption in continuum mechanics is that we can characterise the deformation of the body B with a (possibly piecewise) continuous function $\vec{\phi}$ called a deformation map. The deformation map sends a point P in the reference configuration with position vector \mathbf{x} to a point $\vec{\phi}(P)$ in the deformed configuration with position vector $\vec{\phi}(\mathbf{x})$.

To measure the intensity of deformation (deformation per unit length) about a material point in a continuous body, a quantity called strain is employed. In general, deformation will not be uniform throughout the whole body. Some line segments will experience extensions, while others will experience contractions. Angles between line segments can change. The strain completely characterises the deformation of the infinitesimal neighbourhood of the point \mathbf{x} . We define the Lagrangian strain tensor γ in terms of the

deformation gradient tensor \mathbf{F} as $\gamma = \frac{1}{2}[\mathbf{F}^T \cdot \mathbf{F} - \mathbf{I}]$, where $\mathbf{F} = \nabla \vec{\phi}$ and \mathbf{I} is the identity tensor. We refer our readers to any standard classical continuum mechanics textbook (eg. Hjelmstad, 2005) for a derivation of this measure from first principles, along with a discussion of vectors and tensors.

We can also express the Lagrangian strain tensor in terms of particle displacements. The displacement vector of a point initially at \mathbf{x} that moves to $\vec{\phi}(\mathbf{x})$ as a result of the deformation is given by \mathbf{u} , as illustrated in figure 3. Accordingly, the deformation gradient is given by $\mathbf{F} = \mathbf{I} + \nabla \mathbf{u}$, where $\nabla \mathbf{u}$ is the displacement gradient tensor. The Lagrangian strain tensor can then be defined in terms of the displacement gradient as $\gamma = \frac{1}{2}[\nabla \mathbf{u} + \nabla \mathbf{u}^T + \nabla \mathbf{u}^T \nabla \mathbf{u}]$, where $\nabla \mathbf{u}^T \equiv [\nabla \mathbf{u}]^T$.

We define a special class of deformations known as affine deformations. These are deformations of the form $\vec{\phi}(\mathbf{x}) = \mathbf{F} \cdot \mathbf{x} + \mathbf{c}$, where \mathbf{F} and \mathbf{c} are constants or functions of time only. The deformation gradient of an affine deformation is given by the tensor \mathbf{F} . As a consequence, all of the deformation and strain tensors associated with an affine deformation are independent of position: the body deforms in a uniform manner. Under an affine deformation,

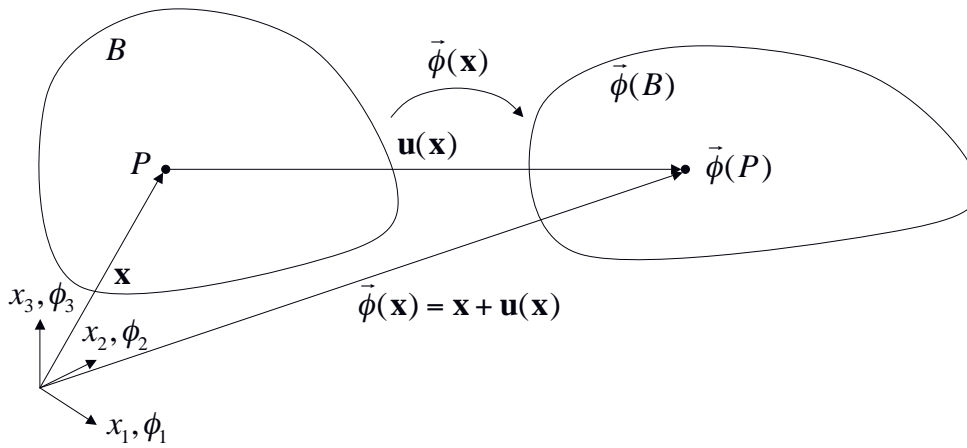


Figure 3: Deformation in terms of displacement.

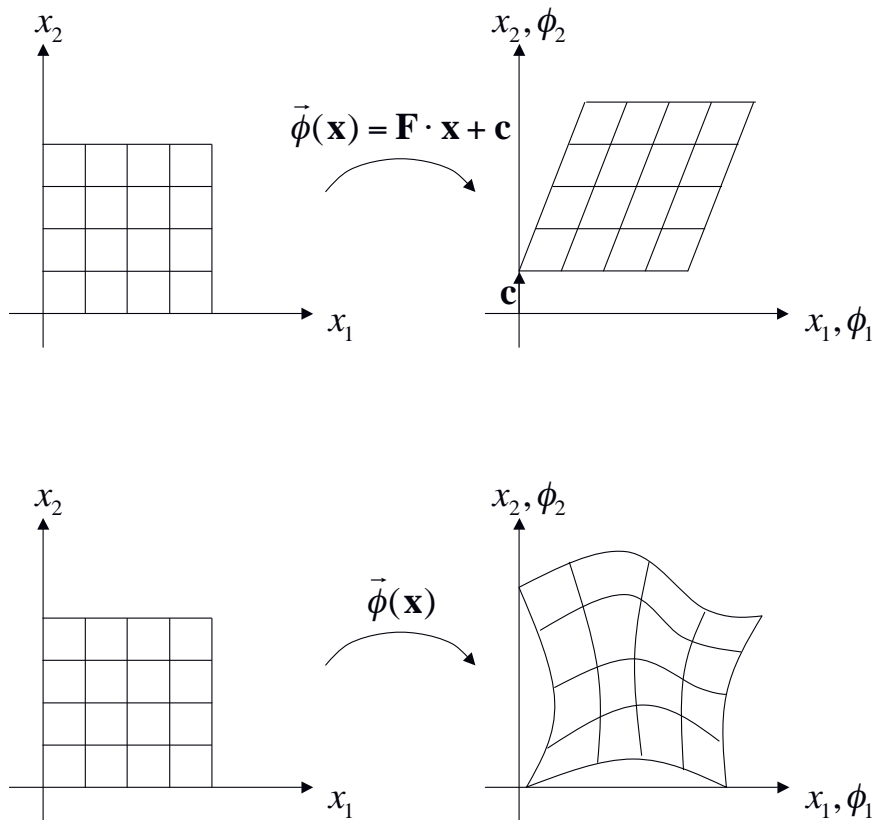


Figure 4: Graphical depictions of an affine (top) and non-affine (bottom) deformation.

material curves that form straight lines in the reference configuration remain straight lines in the deformed configuration (figure 4). Conversely, under a non-affine deformation, material curves that are straight in the reference configuration become curved in the deformed configuration (figure 4).

3 DEFORMATION OF A GRANULAR MATERIAL

Granular materials differ geometrically from continuous bodies due to the heterogeneous characteristics of grains and their possible configurations, and yet it remains convenient to define the strain tensor for a granular material in

terms of the displacement gradient as in continuum mechanics. Before doing so, we must define a representative particle cluster that will form the material point in the continuum representation of the granular material (Tordesillas et al, 2008). For simplicity, we confine our attention to two-dimensional granular assemblies of circular particles of varying sizes. The representative particle cluster comprises a reference particle and its first ring of neighbours, see figure 5.² We then introduce a coordinate system, the origin of which is located at the centre of the reference particle. The vector \mathbf{l}^c that

² This analysis can be extended to spherical particles in three dimensions, however, this extension is beyond the scope of this paper.

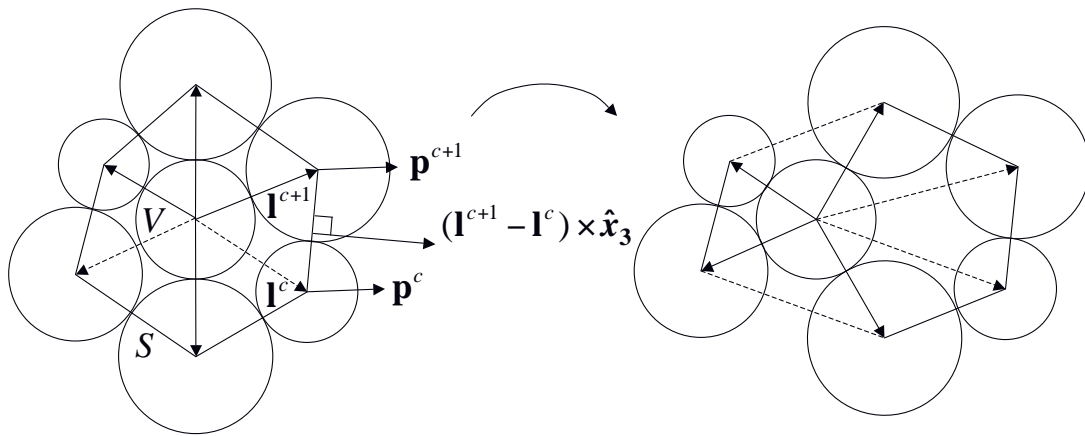


Figure 5: A non-affine deformation of a cluster of seven circular particles in two dimensions.

joins the centre of the reference particle to the centre of its c^{th} neighbour is called a branch vector. The end points of the branch vectors joining the reference particle to its immediate neighbours correspond to the vertices of a Delaunay polygon for the reference particle.³ The Delaunay polygon has boundary S and area V . We define an outwards unit normal vector on the c^{th} edge of the Delaunay polygon by $e_{ijk} (I_k^{c+1} - I_k^c)$ or $(I^{c+1} - I^c) \times \hat{x}_3$, where e_{ijk} is the Levi-Civita symbol, defined by:

$$e_{ijk} = \begin{cases} 0 & \text{for } i = j, j = k \text{ or } k = i \\ +1 & \text{for } (i, j, k) \in \{(1, 2, 3), (2, 3, 1), (3, 1, 2)\} \\ -1 & \text{for } (i, j, k) \in \{(1, 3, 2), (3, 2, 1), (2, 1, 3)\} \end{cases} \quad (1)$$

and \times denotes the cross product.

Let \mathbf{u} be the displacement vector of the reference particle and \mathbf{u}^c be the displacement vector of the c^{th} neighbour. Then the relative displacement vector \mathbf{p}^c describes the displacement of the c^{th} neighbour in relation to the reference particle, and is defined as:

$$\mathbf{p}_i^c = \mathbf{u}_i^c - \mathbf{u}_i + e_{ij3} I_j^c \omega \quad \text{or} \quad \mathbf{p}^c = \mathbf{u}^c - \mathbf{u} + \mathbf{I}^c \times \omega \hat{x}_3 \quad (2)$$

where ω is the angle of rotation of the reference particle. This definition encapsulates an important degree of freedom in granular materials that is absent in classical continua. Note this internal rotation ω is distinct from the macroscopic rotation of the material point that corresponds to the representative particle cluster.

We now derive a measure of strain for a granular material. Consider a continuous displacement field, \mathbf{u} , given for a continuous body. Let V be the area of the body, S its boundary, and \mathbf{n} the outward unit

normal on S . By the divergence theorem in the plane, the volumetric average $\overline{\nabla \mathbf{u}}$ can be expressed as an integral on S :

$$\overline{u_{ij}} = \frac{1}{V} \iint_V u_{ij} dV = \frac{1}{V} \int_S u_i n_j dS \quad (3)$$

where $\overline{u_{ij}}$ are the components of $\overline{\nabla \mathbf{u}}$.

Essentially, we calculate the total change in shape of the body by considering the distances and directions in which the boundary displaces. We then divide by the initial area V of the body to give the average displacement gradient. This defines a new strain tensor, which we can apply to a particle and its first ring of neighbours. The components of the strain tensor, defined for a reference particle, are given by:

$$\varepsilon_{ij} = \frac{1}{V} \int_S p_i n_j dS = \frac{1}{2V} \sum_{c \in B} (p_i^c + p_i^{c+1}) e_{jk3} (I_k^{c+1} - I_k^c) \quad (4)$$

where p_i is a linear interpolation of the p_i^c vectors and the sum is taken anticlockwise over the set B of branch vectors associated with the reference particle.

Since this strain tensor is independent of position (ie. a constant tensor or a function of time), it describes an affine deformation, regardless of whether or not the individual motions of particles adhere to the strict linearity constraints of an affine deformation. This has significant implications. Consider the following scenario: we vertically compress a cluster of seven rigid particles until it deforms, as illustrated in figure 5. Initially, the three particles comprising the central column are aligned. But in order for the cluster to deform, the three central particles must diverge from their initial alignment so that their centres are no longer situated along a straight line. This constitutes a non-affine deformation. However, the strain tensor that we have just defined does not register the non-affinity of this buckling event. Failure to register non-affinity is problematic since non-affinity is associated with a key mechanism in granular systems called force chain buckling (Tordesillas et al, 2008). Experimental studies have shown that force chain buckling governs shear banding, which is regarded as the "signature" of granular media (Tordesillas et

³ The Delaunay-network in two-dimensional Euclidean space is dual to the Dirichlet tessellation. The plane can be partitioned into polygonal domains or Dirichlet-cells such that each Dirichlet-cell contains exactly one grain and every point in a given Dirichlet-cell has a shorter or equal tangent to that grain than to any other grain. If the Dirichlet-cells of two grains have a common edge, the two grain centres are connected with a branch vector. These branch vectors form the Delaunay-network of the assembly (Oda & Iwashita, 2005).

al, 2009; Rechenmacher, 2006; Oda et al, 2004). Once a shear band is fully developed, it effectively splits the material into parts that slide past one another in rigid body motion (Mueth et al, 2000). At this point the material can no longer sustain any load and is said to have failed.

We can capture such non-affine deformation by introducing a new measure to supplement the strain tensor. The difference $\Delta \mathbf{p}^c$ between the actual relative displacement \mathbf{p}^c of the c^{th} neighbour and the displacement $\boldsymbol{\varepsilon} \cdot \mathbf{l}^c$ implied by the strain tensor is:

$$\Delta \mathbf{p}^c = \mathbf{p}^c - \boldsymbol{\varepsilon} \cdot \mathbf{l}^c \tag{5}$$

We define a scalar measure of non-affine deformation associated with the deformation of a particle cluster, comprising a particle and its first ring of neighbours, as:

$$\begin{aligned} \Delta^\varepsilon &= \frac{1}{V} \int_S |\Delta \mathbf{p}| dS = \frac{1}{2V} \sum_{c \in B} (|\Delta \mathbf{p}^{c+1}| + |\Delta \mathbf{p}^c|) |\mathbf{l}^{c+1} - \mathbf{l}^c| \\ &= \frac{1}{2V} \sum_{c \in B} |\Delta \mathbf{p}^c| (|\mathbf{l}^{c+1} - \mathbf{l}^c| + |\mathbf{l}^c - \mathbf{l}^{c-1}|) \end{aligned} \tag{6}$$

This measure is defined for the reference particle and captures the deviations of the relative displacements of neighbouring particles from those displacements implied by the strain tensor. The measure is dimensionless, and therefore independent of particle cluster size.

4 EXAMPLE PROBLEMS

Computed below are the strain tensors and measures of non-affine deformation for two common modes of deformation in two dimensions.

4.1 Example 1 – affine deformation

Consider a cluster of seven circular, rigid particles of unit diameter, as shown in figure 6.

The branch vectors joining the reference particle to its neighbours are given by:

$$\begin{aligned} \mathbf{l}^1 &= (1, 0), \quad \mathbf{l}^2 = \left(\frac{1}{2}, \frac{\sqrt{3}}{2}\right), \quad \mathbf{l}^3 = \left(-\frac{1}{2}, \frac{\sqrt{3}}{2}\right), \\ \mathbf{l}^4 &= (-1, 0), \quad \mathbf{l}^5 = \left(-\frac{1}{2}, -\frac{\sqrt{3}}{2}\right), \quad \mathbf{l}^6 = \left(\frac{1}{2}, -\frac{\sqrt{3}}{2}\right) \end{aligned}$$

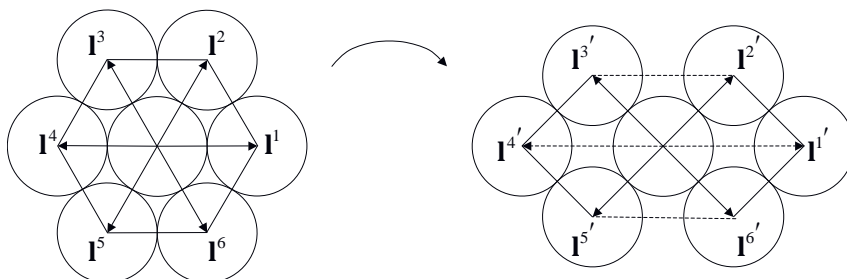


Figure 6: An affine deformation of a seven-particle cluster. Arrows show branch vectors joining the centre of the reference particle to the centres of its neighbours. Dotted lines show virtual contacts.

The images of the branch vectors after deformation are given by:

$$\begin{aligned} \mathbf{l}'^1 &= (\sqrt{2}, 0), \quad \mathbf{l}'^2 = \left(\frac{\sqrt{2}}{2}, \frac{\sqrt{2}}{2}\right), \quad \mathbf{l}'^3 = \left(-\frac{\sqrt{2}}{2}, \frac{\sqrt{2}}{2}\right), \\ \mathbf{l}'^4 &= (-\sqrt{2}, 0), \quad \mathbf{l}'^5 = \left(-\frac{\sqrt{2}}{2}, -\frac{\sqrt{2}}{2}\right), \quad \mathbf{l}'^6 = \left(\frac{\sqrt{2}}{2}, -\frac{\sqrt{2}}{2}\right) \end{aligned}$$

The relative displacement vector \mathbf{p}^c of the neighbour c is $\mathbf{l}'^c - \mathbf{l}^c$. Thus, the relative displacement vectors are given by:

$$\begin{aligned} \mathbf{p}^1 &= (\sqrt{2} - 1, 0), \quad \mathbf{p}^2 = \left(\frac{\sqrt{2}}{2} - \frac{1}{2}, \frac{\sqrt{2}}{2} - \frac{\sqrt{3}}{2}\right), \\ \mathbf{p}^3 &= \left(-\frac{\sqrt{2}}{2} + \frac{1}{2}, \frac{\sqrt{2}}{2} - \frac{\sqrt{3}}{2}\right), \quad \mathbf{p}^4 = (-\sqrt{2} + 1, 0), \\ \mathbf{p}^5 &= \left(-\frac{\sqrt{2}}{2} + \frac{1}{2}, -\frac{\sqrt{2}}{2} + \frac{\sqrt{3}}{2}\right), \quad \mathbf{p}^6 = \left(\frac{\sqrt{2}}{2} - \frac{1}{2}, -\frac{\sqrt{2}}{2} + \frac{\sqrt{3}}{2}\right) \end{aligned}$$

The component ε_{11} of the strain tensor can be computed by substituting $i = 1$ and $j = 1$ into equation (4). Then:

$$\begin{aligned} \varepsilon_{11} &= \frac{1}{2V} \left[(p_1^1 + p_1^2)(l_2^2 - l_2^1) + (p_1^2 + p_1^3)(l_2^3 - l_2^2) \right. \\ &\quad + (p_1^3 + p_1^4)(l_2^4 - l_2^3) + (p_1^4 + p_1^5)(l_2^5 - l_2^4) \\ &\quad \left. + (p_1^5 + p_1^6)(l_2^6 - l_2^5) + (p_1^6 + p_1^1)(l_2^1 - l_2^6) \right] \\ &= \sqrt{2} - 1 \end{aligned}$$

The other components can be computed in a similar fashion. Thus, the strain tensor has components:

$$\boldsymbol{\varepsilon} = \begin{pmatrix} \sqrt{2} - 1 & 0 \\ 0 & \frac{\sqrt{6}}{3} - 1 \end{pmatrix}$$

For this deformation, we observe that $\mathbf{p}^c - \boldsymbol{\varepsilon} \cdot \mathbf{l}^c = 0$ for all $c \in B$. For example, $c = 1$ gives:

$$\mathbf{p}^1 - \boldsymbol{\varepsilon} \cdot \mathbf{l}^1 = \begin{pmatrix} \sqrt{2} - 1 \\ 0 \end{pmatrix} - \begin{pmatrix} \sqrt{2} - 1 & 0 \\ 0 & \frac{\sqrt{6}}{3} - 1 \end{pmatrix} \begin{pmatrix} 1 \\ 0 \end{pmatrix} = \begin{pmatrix} 0 \\ 0 \end{pmatrix}$$

Hence, the relative displacement implied by the strain tensor matches the actual relative displacement of the neighbour c . According to equation (6), it

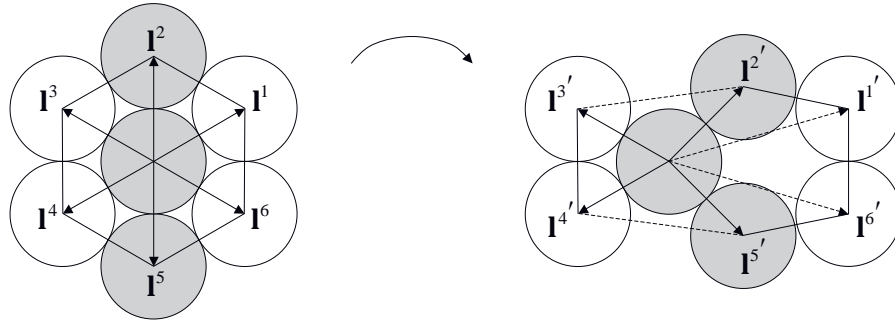


Figure 7: A seven-particle force chain buckling model. Shaded (unshaded) particles are force chain (weak network) particles. Arrows show branch vectors joining the centre of the reference particle to the centres of its neighbours. Dotted lines show virtual contacts.

follows that $\Delta^\varepsilon = 0$. Hence, this deformation is an affine deformation.

4.2 Example 2 – a non-affine deformation of a seven-particle cluster

In this example, we consider the buckling of a force chain under lateral confinement from its weak network neighbours. The particles are assumed to be rigid and of unit diameter, as shown in figure 7.

The branch vectors joining the centre of the reference particle to the centres of its neighbours are given by:

$$\mathbf{I}^1 = \left(\frac{\sqrt{3}}{2}, \frac{1}{2} \right), \quad \mathbf{I}^2 = (0, 1), \quad \mathbf{I}^3 = \left(-\frac{\sqrt{3}}{2}, \frac{1}{2} \right),$$

$$\mathbf{I}^4 = \left(-\frac{\sqrt{3}}{2}, -\frac{1}{2} \right), \quad \mathbf{I}^5 = (0, -1), \quad \mathbf{I}^6 = \left(\frac{\sqrt{3}}{2}, -\frac{1}{2} \right)$$

The images of the branch vectors after deformation are given by:

$$\mathbf{I}^{1'} = \left(\frac{\sqrt{2}}{2} + \sqrt{1 - \left(\frac{1 - \sqrt{2}}{2} \right)^2}, \frac{1}{2} \right), \quad \mathbf{I}^{2'} = \left(\frac{\sqrt{2}}{2}, \frac{\sqrt{2}}{2} \right),$$

$$\mathbf{I}^{3'} = \left(-\frac{\sqrt{3}}{2}, \frac{1}{2} \right), \quad \mathbf{I}^{4'} = \left(-\frac{\sqrt{3}}{2}, -\frac{1}{2} \right),$$

$$\mathbf{I}^{5'} = \left(\frac{\sqrt{2}}{2}, -\frac{\sqrt{2}}{2} \right), \quad \mathbf{I}^{6'} = \left(\frac{\sqrt{2}}{2} + \sqrt{1 - \left(\frac{1 - \sqrt{2}}{2} \right)^2}, -\frac{1}{2} \right)$$

From equation (4), the strain tensor can be computed to have components:

$$\boldsymbol{\varepsilon} = \begin{pmatrix} \frac{\sqrt{6}}{6} + \frac{\sqrt{3}}{3} \sqrt{1 - \left(\frac{1 - \sqrt{2}}{2} \right)^2} - \frac{1}{2} & 0 \\ 0 & \frac{\sqrt{2} - 2}{3} \end{pmatrix}$$

From equation (5), the difference between the actual relative displacement of neighbour 2 and the relative displacement of neighbour 2 implied by the strain tensor is:

$$\Delta \mathbf{p}^2 = \mathbf{p}^2 - \boldsymbol{\varepsilon} \cdot \mathbf{I}^2$$

$$= \begin{pmatrix} \frac{\sqrt{2}}{2} \\ \frac{\sqrt{2}}{2} - 1 \end{pmatrix}$$

$$= \begin{pmatrix} \frac{\sqrt{6}}{6} + \frac{\sqrt{3}}{3} \sqrt{1 - \left(\frac{1 - \sqrt{2}}{2} \right)^2} - \frac{1}{2} & 0 \\ 0 & \frac{\sqrt{2} - 2}{3} \end{pmatrix} \begin{pmatrix} 0 \\ 1 \end{pmatrix}$$

$$\approx \begin{pmatrix} 0.71 \\ -0.10 \end{pmatrix}$$

Similarly, the differences between the actual relative displacements of the other neighbours and the relative displacements implied by the strain tensor are:

$$\Delta \mathbf{p}^1 \approx (0.41, 0.10), \quad \Delta \mathbf{p}^2 \approx (0.71, -0.10), \quad \Delta \mathbf{p}^3 \approx (0.41, 0.10),$$

$$\Delta \mathbf{p}^4 \approx (0.41, -0.10), \quad \Delta \mathbf{p}^5 \approx (0.71, 0.10), \quad \Delta \mathbf{p}^6 \approx (0.41, -0.10)$$

From equation (6), the non-affine deformation⁴ can be computed as:

$$\Delta^\varepsilon = \frac{1}{2V} \left[|\Delta \mathbf{p}^1| (|\mathbf{I}^2 - \mathbf{I}^1| + |\mathbf{I}^1 - \mathbf{I}^6|) \right. \\ \left. + |\Delta \mathbf{p}^2| (|\mathbf{I}^3 - \mathbf{I}^2| + |\mathbf{I}^2 - \mathbf{I}^1|) + |\Delta \mathbf{p}^3| (|\mathbf{I}^4 - \mathbf{I}^3| + |\mathbf{I}^3 - \mathbf{I}^2|) \right. \\ \left. + |\Delta \mathbf{p}^4| (|\mathbf{I}^5 - \mathbf{I}^4| + |\mathbf{I}^4 - \mathbf{I}^3|) + |\Delta \mathbf{p}^5| (|\mathbf{I}^6 - \mathbf{I}^5| + |\mathbf{I}^5 - \mathbf{I}^4|) \right. \\ \left. + |\Delta \mathbf{p}^6| (|\mathbf{I}^1 - \mathbf{I}^6| + |\mathbf{I}^6 - \mathbf{I}^5|) \right]$$

$$\approx 1.2$$

5 FURTHER APPLICATIONS

There exist distinct modes of relative motion between the particles in a deforming granular material. To better understand the relative contribution of each of these modes to strain, we consider some decompositions of the strain tensor. Below we present

⁴ In general, force chains can comprise more than three particles. We can apply the measure of non-affine deformation to larger force chains by analysing them in three-particle segments, as was performed in Tordesillas et al (2009) and Tordesillas (2007).

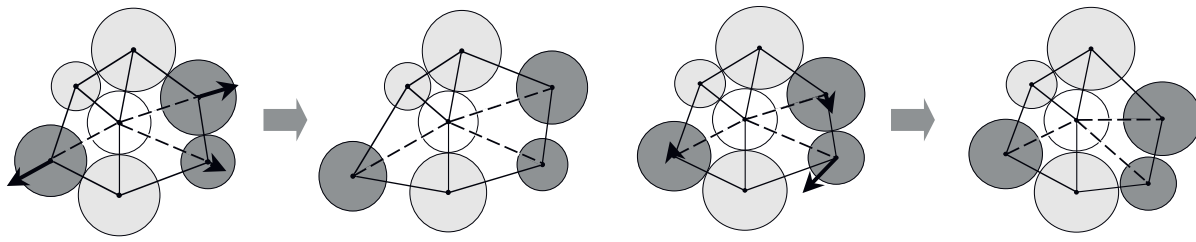


Figure 8: Possible particle motions that lead to different strain contributions. Dark grey particles contribute to the strain and their branch vectors are dotted lines. Light grey particles do not contribute to the strain and their branch vectors are solid lines.

some decompositions that represent contributions from relative motion with respect to in-contact versus out-of-contact neighbours, and motions in the normal versus tangential directions.

The average strain for a particle, ε_{ij}^p , can be decomposed into components describing the relative motion at branch vectors between contacting particles, $\varepsilon_{ij}^{\text{in}}$, and that due to the relative motion at branch vectors between particles that are out of contact, $\varepsilon_{ij}^{\text{out}}$, such that:

$$\varepsilon_{ij}^p = \varepsilon_{ij}^{\text{in}} + \varepsilon_{ij}^{\text{out}} \tag{7}$$

These two strain rate measures are given by:

$$\varepsilon_{ij}^{\text{in}} = \frac{1}{2V^p} \sum_{c \in B^{\text{in}}} (p_i^c + p_i^{c+1}) e_{jk3} (I_k^{c+1} - I_k^c) \tag{8}$$

$$\varepsilon_{ij}^{\text{out}} = \frac{1}{2V^p} \sum_{c \in B^{\text{out}}} (p_i^c + p_i^{c+1}) e_{jk3} (I_k^{c+1} - I_k^c) \tag{9}$$

where the sums are over those branch vectors where the particles are in contact, B^{in} , and those branch vectors where the particles are out of contact, B^{out} , respectively.

Similarly, the successive application of the in-out and normal-tangential decompositions introduces further strain measures: $\varepsilon_{ij}^{\text{in}^n}$ and $\varepsilon_{ij}^{\text{in}^t}$ describing the contribution to the strain at branch vectors between contacting particles due to the relative normal and tangential motion, respectively, and $\varepsilon_{ij}^{\text{out}^n}$ and $\varepsilon_{ij}^{\text{out}^t}$ describing the strain at branch vectors between particles that are out of contact due to the relative normal and tangential motion, respectively. For example, we have:

$$\varepsilon_{ij}^{\text{in}^n} = \frac{1}{2V^p} \sum_{c \in B^{\text{in}}} (p_h^c n_h n_i + p_h^{c+1} n_h n_i) e_{jk3} (I_k^{c+1} - I_k^c) \tag{10}$$

where n_i or \hat{n} is a unit vector normal to the branch vector and $p_h^c n_h$ or $\mathbf{p}^c \cdot \hat{\mathbf{n}}$ denotes the dot product.

As an illustration of these decompositions, we show in figure 8 some particle motions that produce different contributions to the particle volumetric strain $\varepsilon_{\text{vol}}^{\text{in}} = \frac{1}{2} \varepsilon_{ii}^p$, a measure of the change in volume of the material element: if positive, the material is said to have undergone dilatation. By exploring these decompositions, we can get a detailed understanding

of the specific kinds of motion that serve as major contributors to this intriguing phenomenon.⁵

In particular, figure 8(left) shows how a dilative volumetric strain can arise from solely normal motion along out-of-contact branch vectors ($\varepsilon_{ij}^{\text{out}^n}$). Figure 8(right) shows how dilative normal motion and contractive tangential motion from out-of-contact branch vectors ($\varepsilon_{ij}^{\text{out}^n}$, $\varepsilon_{ij}^{\text{out}^t}$) can combine to produce zero volume change in ε_{ij} , $\varepsilon_{ij}^{\text{out}}$ and $\varepsilon_{ij}^{\text{in}}$. A measure of some of these decompositions for the specimen in the simulation⁶ shown in Tordesillas (n. d.) is presented in figure 9. The decompositions evolve with strain distinctly from each other and from the total volumetric strain. Specifically, the contribution from branch vectors between out-of-contact particles begins to dilate before the total volumetric strain, whereas that for in-contact particles continues to undergo compression even after the assembly has commenced dilatation (left plot in figure 9). It can also be observed that $\varepsilon_{\text{vol}}^{\text{in}}$ is due predominantly to normal motions (right plot in figure 9).

6 CONCLUSION

Much of the complex behaviour exhibited by granular materials cannot be described by classical continuum mechanics. In particular, force chain buckling, one of the most interesting and important phenomena associated with the deformation of granular materials, emerges due to the discrete nature of granular systems. The aim of this article was to address the limitations of the classical continuum strain tensor and to give a basic understanding of non-affine deformation in granular materials. The

⁵ A distinctive feature of dense granular materials is Reynolds’ dilatancy; the tendency for a granular material to increase in volume during deformation (For an experiment demonstrating Reynolds’ dilatancy, visit www.grasp.ulg.ac.be/cours/fun/diy/Dilatancy.html). While walking along the beach, Osborne Reynolds puzzled over the apparent whitening or drying up of the sand around his feet. The sand grains beneath his feet experienced shear, causing grains to roll and slide over one another. This motion is akin to a lever action that inherently creates voids between the grains. The surface water drains into these interstitial voids, thus giving the appearance of the sand drying up around Reynolds’ feet.

⁶ These simulations show the temporal evolution of the non-affine deformation of the particle motion.

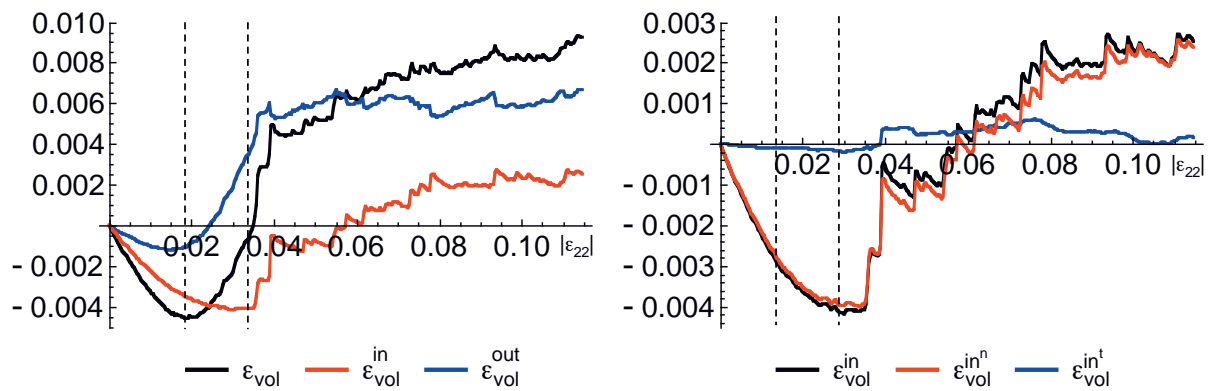


Figure 9: Two possible decompositions of the particle volumetric strain tensor.

worked examples included in this article demonstrate how to compute the non-affinity associated with two common modes of deformation. A code facilitates further study and exploration of the important connection between particle kinematics and strain.

REFERENCES

Behringer, R. P., n. d., "Bob Behringer's Home Page", www.phy.duke.edu/~bob, Duke University.

Duran, J. 2000, *Sands, Powders and Grains: An Introduction to the Physics of Granular Materials*, Springer.

Group of Research and Applications in Statistical Physics, n. d., "Reynolds' dilatancy", www.grasp.ulg.ac.be/cours/fun/diy/Dilatancy.html, Université de Liège.

Hjelmstad, K. D. 2005, *Fundamentals of Structural Mechanics*, USA, Springer, pp. 57-93.

Kuhn, M. & Bagi, K. 2002, "Particle rotations in granular materials", 15th ASCE Engineering Mechanics Conference, New York.

Low Temperature Behringer (LTB) Group, 2004, "Behringer's Nonlinear Flow Group Page", www.phy.duke.edu/research/cm/behringer, Duke University.

Majmudar, T. S. & Behringer, R. P. 2005, "Contact force measurements and stress induced anisotropy in granular materials", *Nature*, Vol. 435, pp. 1079-1082; see also "Colorful math reveals how forces transmit through granular materials" at www.physorg.com/news4686.html.

Mueth, D. M., Debregeas, G. F., Karczmar, G. S., Eng, P. J., Nagel, S. R. & Jaeger, H. M. 2000, "Signatures

of granular microstructure in dense shear flows", *Nature*, Vol. 406, No. 6794, pp. 385-389.

Oda, M. & Iwashita, K. 2005, *Mechanics of granular materials: an introduction*, Balkema, Netherlands.

Oda, M., Takemura, T. & Takahashi, M. 2004, "Microstructure in shear band observed by microfocus X-ray computed tomography", *Geotechnique*, Vol. 54, No. 8, pp. 539.

Rechenmacher, A. 2006, "Grain-scale processes governing shear band initiation and evolution in sands", *J. Mech. Phys. Solids*, Vol. 54, No. 1, pp. 2245.

Tordesillas, A. 2007, "Force chain buckling, unjamming transitions and shear banding in dense granular assemblies", *Philosophical Magazine*, Vol. 87, No. 32, pp. 4987-5016.

Tordesillas, A., n. d., "The micromechanics of granular material: Sample projects for 2009", www.mgm.ms.unimelb.edu.au/projects2009.php, The University of Melbourne.

Tordesillas, A. & Arber, D. 2005, "Capturing the S in segregation: a simple model of flowing granular mixtures in rotating drums", *International Journal of Mathematical Education in Science and Technology*, Vol. 36, No. 8, pp. 861-877.

Tordesillas, A., Muthuswamy, M. & Walsh, S. D. C. 2008, "Mesoscale measures of nonaffine deformation in dense granular assemblies", *Journal of Engineering Mechanics*, Vol. 134, No. 12, pp. 1095-1113.

Tordesillas, A., Zhang, J. & Behringer, R. P. 2009, "Buckling force chains in dense granular assemblies: physical and numerical experiments", *Geomechanics and Geoengineering*, Vol. 4, No. 1, pp. 3-16.



ANTOINETTE TORDESILLAS

Antoinette Tordesillas is currently an Associate Professor and Reader in Mathematics and Statistics at the University of Melbourne. She has worked at the interface of engineering mechanics, physics and mathematics since her honours year at university. Her current research activities in micromechanics of granular materials involve the development and application of new methodologies, in part stemming from other domains, ie. complex networks, micromechanics, dynamical systems and structural mechanics. Her group has ongoing collaborations with experimentalists from NASA, US Army, APEC Centre for Earthquake Simulation, Duke University and MIT. All of these projects involve undergraduate students from engineering and science.



DAVID KIRSZENBLAT

David Kirszenblat is an undergraduate student at the University of Melbourne. He is currently enrolled in a Bachelor of Science and a Bachelor of Arts, and is majoring in pure mathematics, physics, philosophy and French. He recently completed a vacation scholarship project on the micromechanics of granular media under the supervision of A/Prof Antoinette Tordesillas. His project involved the mastering of concepts described in this paper.



CHRISTINE MANGELSDORF

Christine Mangelsdorf is a lecturer in the Department of Mathematics and Statistics at the University of Melbourne. She has taught Vector Calculus to second-year level undergraduate engineering, mathematics and physics students for the past 10 years. She is the organiser of the one-day fair "Real World Mathematics in Action" for Year 11 and 12 students and their teachers, held every two years at the University of Melbourne. She is also the Treasurer for the Victorian Branch of ANZIAM (Australian and New Zealand Industrial and Applied Mathematics).